

# $g_1$ at low $x$ and low $Q^2$ with Polarized $ep$ Colliders

Steven D. Bass<sup>†</sup>

*Physik Department, Technische Universität München,  
D-85747 Garching, Germany*

Albert De Roeck<sup>‡</sup>

*CERN, CH-1211 Geneva 23, Switzerland*

## Abstract

Measurements of  $g_1$  at low  $x$  and low  $Q^2$  are expected to provide a sensitive probe of the transition from Regge to perturbative QCD dynamics, offering a new testing ground for models of small  $x$  physics. We discuss the potential of polarized  $ep$  colliders (Polarized HERA and eRHIC) to investigate this physics — varying  $Q^2$  between 0.01 and 1 GeV<sup>2</sup> — and to constrain the high-energy part of the Drell-Hearn-Gerasimov sum-rule for polarized photoproduction.

---

<sup>†</sup>steven.bass@cern.ch

<sup>‡</sup>albert.de.roeck@cern.ch

# 1 Introduction

The HERA measurements of the proton structure function  $F_2(x, Q^2)$  at low  $x$  and low  $Q^2$  (less than  $1 \text{ GeV}^2$ ) mark the transition between Regge “confinement physics” and perturbative QCD. For fixed  $Q^2$  up to  $0.65 \text{ GeV}^2$  the measured large  $s_{\gamma p} \sim Q^2/x$  behaviour of  $F_2$  is consistent with the expectations of Regge phenomenology [1]. For values of  $Q^2$  greater than  $1 \text{ GeV}^2$  the  $F_2$  data is well described [2] by DGLAP evolution [3] and rises faster with decreasing  $x$  than the soft Regge prediction. The “transition region” between photoproduction and deep inelastic scattering and the onset of perturbative QCD is a subject of much current interest [4, 5].

The small  $x$  behaviour of nucleon structure functions  $f(x, Q^2)$  is often described in terms of an effective intercept  $\lambda$  ( $f(x, Q^2) \sim x^{-\lambda}$  at small Bjorken  $x$ ) which changes between 0.1 and 0.4 for unpolarized data. In the transition from photoproduction to deep inelastic values of  $Q^2$  much larger changes are expected in the effective intercept for the  $g_1$  spin dependent structure function compared to the spin independent structure function  $F_2$  – see Section 2 below. In this paper we discuss the potential of Polarized  $ep$  Colliders (Polarized HERA and eRHIC) [6, 7, 8] to measure the spin dependent part of the total photon–nucleon cross-section for photon virtualities  $Q^2$  between 0 and  $1 \text{ GeV}^2$ . These measurements would help constrain the high-energy part of the Drell-Hearn-Gerasimov sum-rule [9] for spin dependent photoproduction and impose new constraints on theoretical models which aim to describe the transition from soft to hard physics at small  $x$ . Open questions are: At which  $Q^2$  does the effective intercept for  $g_1$  start to grow ? What is the rate of growth with increasing  $Q^2$  ? Where in  $Q^2$  will perturbative QCD start to describe future  $g_1$  data at small  $x$  ?

The physics program of the Polarized HERA project is documented in [6] and Polarized eRHIC is discussed in [7]. HERA  $ep$  collisions are at a centre of mass (CMS) energy  $300 \text{ GeV}$ , while eRHIC is foreseen to operate at a CMS energy of  $100 \text{ GeV}$ . The low  $Q^2$  measurements would complement deep inelastic measurements of  $g_1$  at low  $x$  (extend to low  $Q^2$ ) and studies of  $\Delta g$  and spin dependence of diffraction. The expected electron and proton beam polarizations are  $P_e = P_p = 70\%$  and the integrated luminosity is  $\mathcal{L} = 500 \text{ pb}^{-1}$  (HERA) or  $\mathcal{L} = 4 \text{ fb}^{-1}$  (eRHIC) after several years of data taking. Hence one expects [8] to be able to measure the electron-proton spin asymmetry at small  $x$  (less than about 0.05) to a precision  $\delta A \simeq 0.002 - 0.0001$  or better in deep inelastic scattering. Recent ideas on using polarized deuterons may give access to  $g_1^p$  and  $g_1^n$  separately.

In Section 2 we outline the key physics issues. Experimental aspects are discussed in Section 3. Section 4 contains an estimate of the possible asymmetries. Finally, in Section 5 we conclude.

## 2 The transition region

We first recall what is known about the transition region in  $F_2$ . In the HERA kinematical region the total  $\gamma^*p$  cross-section is related to  $F_2(x, Q^2)$  by

$$\sigma_{\text{tot}}^{\gamma^*p}(s, Q^2) \simeq \frac{4\pi^2\alpha}{Q^2} F_2(x, Q^2) \quad (1)$$

where  $s \simeq Q^2/x$  is the CMS energy squared for the  $\gamma^*p$  collision. For  $Q^2 < 0.65 \text{ GeV}^2$  and  $s \geq 3 \text{ GeV}^2$  the  $\sigma_{\text{tot}}$  data [10, 11, 12] seems to be well described by a combined Regge and Generalized Vector Meson Dominance (GVMD) motivated fit. The ZEUS Collaboration used the 4 parameter fit [12]

$$\sigma_{\text{tot}}^{\gamma^*p}(s, Q^2) = \left( \frac{M_0^2}{M_0^2 + Q^2} \right) \left( A_R s^{\alpha_R - 1} + A_P s^{\alpha_P - 1} \right) \quad (2)$$

to describe the low  $Q^2$  region, with  $A_R = 147.8 \pm 4.6 \mu\text{b}$ ,  $\alpha_R = 0.5$  (fixed),  $A_P = 62.0 \pm 2.3 \mu\text{b}$ ,  $\alpha_P = 1.102 \pm 0.007$  and  $M_0^2 = 0.52 \pm 0.04 \text{ GeV}^2$ . For  $Q^2$  larger than  $1 \text{ GeV}^2$  the HERA data on  $F_2$  seems to be well described by DGLAP evolution. Parametrising  $F_2 \sim Ax^{-\lambda}$  at small  $x$  the effective intercept  $\lambda$  is observed to grow from  $0.11 \pm 0.02$  at  $Q^2 = 0.3 \text{ GeV}^2$  to  $0.18 \pm 0.03$  at  $Q^2 = 3.5 \text{ GeV}^2$ ,  $0.31 \pm 0.02$  at  $35 \text{ GeV}^2$  and increases with increasing  $Q^2$  [11, 10, 13].

What do we expect for  $g_1$  ?

Let  $\sigma_A$  and  $\sigma_P$  denote the  $\gamma p$  total cross-section for photons polarized antiparallel  $\sigma_A$  and parallel  $\sigma_P$  to the spin of the proton. In HERA kinematics  $g_1$  is related to  $(\sigma_A - \sigma_P)$  by

$$(\sigma_A - \sigma_P) \simeq \frac{4\pi^2\alpha}{p \cdot q} g_1 \quad (3)$$

where  $p$  and  $q$  are the proton and photon four-momenta respectively. The Regge prediction for the large  $s_{\gamma p}$  behaviour of  $(\sigma_A - \sigma_P)$  is [14, 15, 16, 17, 18]

$$(\sigma_A - \sigma_P) \sim N_3 s^{\alpha_{a_1} - 1} + N_0 s^{\alpha_{f_1} - 1} + N_g \frac{\ln(s/\mu^2)}{s} + N_{PP} \frac{1}{\ln^2(s/\mu^2)} \quad (4)$$

at large  $s$ . The  $s^{\alpha_{a_1} - 1}$  contribution is isotriplet; the  $s^{\alpha_{f_1} - 1}$ ,  $(\ln s)/s$  and  $1/\ln^2 s$  contributions are isosinglet;  $\mu$  is a typical hadronic scale  $\mu \sim 0.5 - 1 \text{ GeV}$ . The coefficients  $N_3$ ,  $N_0$ ,  $N_g$  and  $N_{PP}$  are to be determined from experiment.

If one makes the usual assumption that the  $a_1$  and  $f_1$  trajectories are straight lines running parallel to the  $(\rho, \omega)$  trajectories, then one finds  $\alpha_{a_1} \simeq \alpha_{f_1} \simeq -0.4$ . This value is within the phenomenological range  $-0.5 \leq \alpha_{a_1} \leq 0$  quoted by Ellis and Karliner [15]. The  $\ln s/s$  term is induced by any vector component to the short range exchange potential [16]. It corresponds to a term in  $g_1$  proportional to  $\ln x$ . Extending the Donnachie-Landshoff-Nachtmann [19] model of soft pomeron exchange to  $g_1$  Bass and Landshoff [17] found that the physics of nonperturbative

two-gluon exchange, which generates the soft pomeron contribution to  $F_2$ , also generates a  $(2 \ln \frac{1}{x} - 1)$  contribution in  $g_1$ . The  $\ln x$  singularity is associated with the non-perturbative gluons emitted collinear with the proton. The  $1/\ln^2 s$  term [18] is associated with a two-pomeron cut. Kuti [20] has recently argued that the signature rule for Pomeron Regge cuts is expected to set  $N_{PP} = 0$ . In this paper we will allow this term to help parametrise any less convergent behaviour of  $(\sigma_A - \sigma_P)$  at large  $s$  which might possibly show up in future data.

A high quality measurement of  $(\sigma_A - \sigma_P)$  at  $Q^2 = 0$  would help to constrain the high-energy part of the Drell-Hearn-Gerasimov sum-rule [9, 21] for spin dependent photoproduction. This sum-rule relates the difference  $(\sigma_A - \sigma_P)$  to the square of the anomalous magnetic moment of the target nucleon and is often quoted in the target-rest frame:

$$(\text{DHG}) \equiv -\frac{4\pi^2\alpha\kappa^2}{2m^2} = \int_{\nu_{th}}^{\infty} \frac{d\nu}{\nu} (\sigma_A - \sigma_P)(\nu). \quad (5)$$

Here  $\nu$  is the LAB energy of the exchanged photon,  $m$  is the nucleon mass and  $\kappa$  is the anomalous magnetic moment. Phenomenological Regge based estimates [22, 23] suggest that  $25 \pm 10 \mu\text{b}$  (about 10%) of the sum-rule may come from  $\sqrt{s_{\gamma p}} > 2.5 \text{ GeV}$  – the highest energy of the present Bonn-Mainz Drell-Hearn-Gerasimov experiment.

It is an open question how far one can increase  $Q^2$  away from the photoproduction limit and still trust Regge theory to provide an accurate description of  $g_1$  in HERA kinematics. It is well known [24] that small  $x$  behaviour of the form  $g_1 \sim x^{-\alpha}$  where  $\alpha < 0$  is unstable to DGLAP evolution [25, 26, 27] and to resummation of  $(\alpha_s \ln^2 \frac{1}{x})^k$  [28, 29, 30, 31] terms at small  $x$  in perturbative QCD. Theoretical studies suggest that the precise shape of  $g_1$  at small  $x$  in deep inelastic scattering is particularly sensitive [31] to the details of the QCD evolution, and might even rise as fast as  $|g_1| \sim \frac{1}{x}$  [28].

Regge theory provides a good fit [1] to the NMC fixed target experiment “small  $x$ ” data [32] ( $0.008 < x < 0.07$ ) on  $F_2^{(p\pm n)}(x, Q^2)$  at deep inelastic  $Q^2$  between 1 and 10  $\text{GeV}^2$ . It does not appear to describe  $g_1$  data in the same kinematical region. Taking  $\alpha_{a_1} \simeq -0.4$  in Eq.(4) yields a Regge prediction  $g_1 \sim x^{0.4}$  at small  $x$ . In contrast, polarized deep inelastic data from CERN [33] and SLAC [34, 35] consistently indicate a strong isotriplet term in  $g_1$  which rises at “small  $x$ ” between 0.01 and 0.1 at  $Q^2 \simeq 5 \text{ GeV}^2$ . One finds a good fit [36, 22]

$$g_1^{(p-n)} \sim (0.14) x^{-0.5} \quad (6)$$

to the SLAC  $g_1$  data which has the smallest experimental errors. This fit corresponds to an effective intercept  $\alpha_{a_1}(Q^2) \simeq +0.5$  for this kinematical region — between 0.5 and 1.0 greater than the soft Regge prediction if we take the phenomenological range  $-0.5 \leq \alpha_{a_1} \leq 0$  [15]. It is interesting to note that a large “small  $x$ ” contribution

to  $g_1^{(p-n)}$  in this kinematics is almost necessary [37] to accommodate the large area under the Bjorken sum-rule for  $g_1^{(p-n)}$  [38] — a non-perturbative constraint. It will be interesting to see how well the fit (6) describes future  $g_1$  data at smaller Bjorken  $x$ . For  $g_1^{(p+n)}$  the situation is less clear. The SLAC data indicates that  $g_1^{(p+n)}$  is small and consistent with zero in the  $x$  range  $0.01 < x < 0.05$ . Theoretically, one expects here a sum of different exchange contributions with possibly different signs.

To summarise, the change in the effective intercepts for  $g_1^{(p\pm n)}$  between photo-production and deep inelastic scattering, say at  $Q^2 \sim 5\text{GeV}^2$ , could be as large as one — a factor of 5 bigger than the effect observed in  $F_2$ .

### 3 Experimental aspects

The lowest  $Q^2$  values at large  $1/x$  can be reached in collider type of lepton-hadron experiments. HERA is presently the only high energy  $ep$  collider, with a 27.5 GeV electron and 820 (920) GeV proton beam, leading to interactions with  $\sqrt{s} = 300$  (314) GeV. Presently the collider experiments at HERA record unpolarized  $ep$  collisions. In fall 2000 spin rotators will be installed in the electron ring converting the transverse polarization of the electron beam, which builds up due to the Sokolov-Ternov [39] effect, into a physics-wise more interesting longitudinal polarization. Studies are being made to provide in future also a polarized proton beam at HERA [40] which would enable polarized  $ep$  and thus also polarized  $\gamma p$  collisions. In 2000 HERA will also undergo a luminosity upgrade [41], which for the experiments has the consequence that magnets are inserted close to the interaction point, and the beam-line and beam optics will change. In this mode HERA is expect to deliver a luminosity in the range of 150-200  $\text{pb}^{-1}/\text{year}$  per experiment.

At BNL a new project, called eRHIC, is under study[7]. It is proposed to add a polarized electron ring/accelerator to the already existing and recently commissioned  $pp/AA$  machine RHIC. Polarized proton beams are already planned for RHIC. Hence polarized  $ep$  collisions at a CMS energy of about 100 GeV will be possible at eRHIC (10 GeV  $e$  on 250 GeV  $p$ ).

If HERA is fully polarized, event samples of the order of 100 – 500  $\text{pb}^{-1}$  are expected to be collected, with expected beam polarizations  $P_e = P_p = 0.7$ . For eRHIC we will assume the same beam polarizations but a higher total integrated luminosity, namely of order of 1  $\text{fb}^{-1}/\text{year}$ .

As discussed above, in spin physics non-singlet and singlet contribution decomposition is important, and for that reason it is crucial to have also access to the spin structure functions of the neutron. The original idea at HERA was to use additionally  $\text{He}^3$  beams, which strongly resemble the protons from the spin acceleration point of view. Recently, the idea to use deuterons has re-emerged. High energy polarized deuteron beams have in fact several advantages compared to protons. Due

to the much smaller gyromagnetic anomaly  $G = (g - 2)/2$  (1.79 for protons,  $-0.14$  for deuterons) it will be easier to accelerate a polarized deuteron beam over the depolarizing resonances, and the beams are less susceptible to spin distortions[42]. The known disadvantage is that with current magnet technology it is not possible to use spin rotators to rotate the transverse deuteron spin into a longitudinal one. Novel ideas for rotating the spin based on magnetic  $rf$  dipole fields could however change this situation significantly. Here we will assume that high energy polarized deuteron beams can be made and stored (in HERA up to 460 GeV/nucleon and eRHIC up to 125 GeV/nucleon), with the same luminosity and same polarization as for protons (which does not seem unfeasible [43]). Note that if tagging of the spectator particle, i.e. the particle which did not undergo an interaction, with high efficiency and kinematical coverage could be achieved, by means of proton spectrometers or neutron calorimeters down the beamline (also termed “the forward direction”), one could measure directly both  $ep$  and  $en$  scattering contributions separately using event samples with either a proton or neutron spectator tagged. Hence one can measure separately but simultaneously  $g_1^p$  and  $g_1^n$ , as already proposed in [44]. Some coverage for the detection of forward protons and neutrons is already available at HERA. An excellent, quasi-complete coverage of the forward direction is foreseen in the first ideas for a detector at eRHIC [45].

### 3.1 Photoproduction

Photoproduction, i.e.  $Q^2 = 0$ , cross-sections can be measured in  $ep$  collisions at a collider at high  $\sqrt{s_{\gamma p}}$  energies. In fact the dominant processes in  $ep$  collisions are  $\gamma p$  interactions where the photon is on mass shell. The electron is scattered under approximately zero degrees with respect to the electron beam direction, which means that it remains in the beampipe. The energy of the scattered electron  $E'_e$  is however reduced to  $E'_e = E_e - E_\gamma$ , with  $E_e$  the incident electron energy and  $E_\gamma$  the emitted photon energy. The HERA machine magnets in the beamline, which steer the beam into a closed orbit, act as a spectrometer on these off-momentum electrons, and they will be kicked out of the beam orbit. The experiments H1 and ZEUS have installed calorimeters to detect these kicked out electrons along the beamline. In case of H1 calorimeters (stations) are installed at three locations: at 8 m, 30 m and 44 m distance from the interaction point [46]. The stations accept (tag) electrons from different momentum ranges, which correspond to  $\sqrt{s_{\gamma p}}$  ranges of 280-290 GeV, 150-250 GeV and 60-115 GeV respectively. At the central energy value of each region the acceptance of these devices amounts to 20%, 80% and 70% respectively.

Eq.(8) below shows that the  $\gamma p$  cross section is large, of order of hundreds of microbarns. The photon energy spectrum emitted from an electron beam follows the Weizsäcker-Williams approximation [47]. An integrated  $ep$  luminosity at HERA

of  $1 \text{ pb}^{-1}$  can yield about 1500K  $\gamma p$  events in each of the 30 m and 44 m stations, and about 10 times less in the 8 m station.

In the small asymmetry approximation the error on the asymmetries,  $\delta A$ , can be calculated as  $1/(P_e P_p \sqrt{N})$ . Due to data-taking bandwidths and trigger challenges presently not all tagged  $\gamma p$  events are recorded. Assuming a data taking rate of 2 Hz for these events, also in future, leads to about 40 M events/year giving a reachable precision on the  $ep$  asymmetry  $\delta A = 1/(P_e P_p \sqrt{N}) = 0.0003$ . It is however not excluded that novel techniques in triggering, data-taking and on-line analysis will become available, which would allow to collect or use the information of all produced events, amounting to approximately 15,000M events in total for the three stations in a period of 3 to 5 years. This would lead to maximal reachable precisions of  $\delta A = 3 \cdot 10^{-5}$  for a measurement at the 30m and the 44m station, and  $\delta A = 10^{-4}$  for a measurement at the 8m station.

Since the  $\gamma p$  asymmetries are measured via  $ep$  collisions the polarization of the photon beam will be reduced by a so called depolarization factor  $D = y(2-y)/(y^2 + 2(1-y))$  with  $y = s_{\gamma p}/s_{ep}$ . For the three stations the measurements are at  $y = 0.09, 0.44$  and  $0.90$ , leading to values of  $D = 0.094, 0.52$  and  $0.98$ . Hence the maximal reachable precision for measuring the  $\gamma p$  asymmetries  $A_1$  using  $ep$  at HERA is  $10^{-4}$  (280-290 GeV),  $6 \cdot 10^{-5}$  (150-250 GeV) and  $3 \cdot 10^{-4}$  (60-115 GeV).

If the same photoproduction tagging techniques as used at HERA can be used at eRHIC, and if the data taking and analysis bandwidth is not preventative, an experiment at this machine could measure the  $\gamma p$  cross section asymmetry with a precision of about a factor three better, in the region  $20 < \sqrt{s_{\gamma p}} < 90 \text{ GeV}$ , complementary to HERA.

Using a deuteron beam one could measure the  $A_1^{p+n}$  asymmetry with the same precision, but for reduced  $\sqrt{s_{\gamma p}}$  regions, namely 40 – 200 GeV at HERA and 14 – 70 GeV at eRHIC. Using spectator tagging the individual  $A_1^p$  and  $A_1^n$  asymmetries can be measured with roughly a factor of two worse precision, compared to  $A_1^{p+n}$ .

After the luminosity upgrade of HERA the present electron taggers for photoproduction events will undergo changes, be partially located at different positions, and have a different acceptance. The regions which are expected to be covered after the upgrade for  $Q^2 = 0$  events are  $70 < \sqrt{s_{\gamma p}} < 150 \text{ GeV}$  and  $210 < \sqrt{s_{\gamma p}} < 265 \text{ GeV}$ , but the precision to measure the asymmetries should be as above.

### 3.2 Low $Q^2$ Region.

The low  $Q^2$ , or transition, region from photoproduction to deep inelastic scattering is investigated presently at the HERA collider for unpolarized  $ep$  collisions by the H1 and ZEUS experiments. Similarly to the photoproduction events discussed above, the main characteristic of low  $Q^2$  scattering in the HERA LAB frame is the small

but this time non-zero scattering angle of the electron with respect to the beam direction. These electrons will leave the beampipe a few meters after the interaction point. Hence special care has to be taken to detect these electrons with detectors which are closely integrated with the beam-pipe structure of the accelerator.

Fig.1a) shows the kinematics of the scattered electron for HERA. In order to reach small  $Q^2$  values, below  $0.1 \text{ GeV}^2$ , electrons need to be detected with scattering angles of  $1^\circ$  or less.

The standard central detectors of H1 and ZEUS typically detect electrons down to an angle of about 2 degrees, resulting in a region of good acceptance for  $Q^2$  values above a few  $\text{GeV}^2$ . In order to reach smaller values both experiments have added to the central detector a special “beam-pipe calorimeter” and “tracker” (BPC and BPT; ZEUS) and “Very Low  $Q^2$ ” detector (VLQ; H1). These detectors have however a limited azimuthal coverage. ZEUS has already used the BPC and BPT detectors to present measurements of  $F_2$  based on 1997 data. The measurements cover the region of  $Q^2$  down to  $0.045 \text{ GeV}^2$  [48]. The VLQ detector of H1 [49] consists of a silicon tracker and Tungsten-scintillator calorimeter and was commissioned in 1998. The VLQ is expected to provide measurements down to  $0.03\text{-}0.05 \text{ GeV}^2$ . In this paper we will assume one can detect electrons down to  $10 \text{ mrad}$ , which is slightly better than presently available with the VLQ and BPT. With present standard methods for event kinematics reconstruction the region in Bjorken  $y$  of  $0.1 < y < 0.7$  can be safely measured. Further we will restrict the measured  $Q^2$  region from  $0.03 \text{ GeV}^2$  to  $1.5 \text{ GeV}^2$  in  $Q^2$ . Resolution and event statistics considerations for polarized measurements lead to the possible binning in  $Q^2$  and  $s_{\gamma p}$  given in Table 1. Using the parametrization of [12] in this region, the number of events per bin is of the order of  $1 - 2 \cdot 10^6$  for an integrated luminosity of  $100 \text{ pb}^{-1}$ . One interesting aspect to be studied with the data is the energy dependence of the unpolarized cross section. With these data samples and assuming that the systematic errors on the measurements will be mostly correlated, one will measure the exponents  $\alpha_R, \alpha_P$  in Eq.(2) with an unprecedented precision of better than  $10^{-3}$ .

The luminosity upgrade at HERA will effectively reduce the acceptance for scattered electrons for low  $Q^2$  DIS events, due to the focussing magnets in the detectors, close to the interaction point, and measurements in the kinematical range presently covered by the VLQ are not foreseen. Hence, for the low  $Q^2$  measurement a new way of detecting and measuring DIS events within the upgraded environment has to be found, in order that this measurement can benefit from the luminosity upgrade, which would give approximately  $150 \text{ pb}^{-1}/\text{year}$ . Without these focussing magnets (but still some less aggressive improvements compared to the present luminosity upgrade [50]) HERA could still accumulate between  $50$  and  $100 \text{ pb}^{-1}/\text{year}$ . We assume here that this measurement will or can be made at a later stage in a lower luminosity configuration, and assume a total luminosity of  $100 \text{ pb}^{-1}$ , corresponding to 1-2 years



of data taking. This leads to a reachable precision  $\delta A = 1/(P_e P_p \sqrt{N}) = 0.002-0.001$  per bin. When less bins are chosen and/or a solution is found to make this measurement within the upgraded luminosity program, the ultimate sensitivity can increase with a factor of 3 to 4. Note that the true  $\gamma^*p$  asymmetries are reduced due to the depolarization factor  $D$ , which lowers the effective sensitivities by values which range from 0.17 to 0.72. Hence we take  $\delta A_1 = 0.002$  as a typical reachable value for the precision of the  $\gamma^*p$  asymmetry measurement.

When running HERA at lower energies (e.g.  $E_p = 200$  GeV and  $E_e = 15$  GeV), one could also reach  $s_{\gamma p}$  values which are a factor of 3 lower than the ones in Table 1. Note however that the sensitivity will reduce by about a factor 5 to 10 or so, due to the reduced luminosity of HERA at these energies, and the fact that it is unlikely that data at such energies would be taken for a full year.

For eRHIC access to the low  $Q^2$  region becomes easier, as shown in Fig.1b). Due to the different beam energies electrons from DIS events with a  $Q^2$  of 0.1 GeV<sup>2</sup> scatter at an angle of 2 degrees or more, which allows them to be accepted within the central detector. Special beam-pipe calorimeters and trackers are only required for the region  $0.01 < Q^2 < 0.1$  GeV<sup>2</sup>. If also at eRHIC scattered electrons can be tagged down to 10 mrad, then  $Q^2$  values down to 0.003 GeV<sup>2</sup> can be reached. The higher luminosity of RHIC and larger azimuthal acceptance will allow one to measure the asymmetries 10-15 times more precisely, but in a kinematic range where, for the same  $Q^2$ ,  $x$  is 10 times larger than for HERA.

As for the photoproduction case, using a deuteron beam one could measure the  $A_1^{p+n}$  asymmetry with the same precision, but for reduced  $s_{\gamma p}$  regions, i.e. for  $x$  values a factor two larger than those accessible with proton beams for the same  $Q^2$ . In case spectator tagging is available  $A_1^p$  and  $A_1^n$  asymmetries could be measured simultaneously with a factor of about two worse precision.

## 4 Estimating asymmetries

We now estimate the spin asymmetry  $A_1 = (\sigma_A - \sigma_P)/(\sigma_A + \sigma_P)$  at low  $Q^2$  and discuss the measurement potential of Polarized HERA and eRHIC.

### 4.1 Photoproduction

In Fig.2 we show the estimate of the real photon asymmetry  $A_1$  from [51, 22]. This estimate was obtained as follows. We took the SLAC E-143 [52] and SMC [33] measurements of  $A_1 = (\sigma_A - \sigma_P)/(\sigma_A + \sigma_P)$  at low  $Q^2$  (between 0.25 and 0.7 GeV<sup>2</sup>) in the ‘‘Regge region’’ ( $\sqrt{s_{\gamma p}} \geq 2.5$  GeV). This low  $Q^2$  data exhibits no clear  $Q^2$  dependence in either experiment. Motivated by this observation and the ZEUS fit (2) to  $F_2(x, Q^2)$  at low  $Q^2$  we assume that  $A_1$  is  $Q^2$  independent for  $Q^2 < 0.7$  GeV<sup>2</sup>.

That is, we conjecture

$$(\sigma_A - \sigma_P)^{\gamma^* p}(s, Q^2) = \left( \frac{M_0^2}{M_0^2 + Q^2} \right) (\sigma_A - \sigma_P)^{\gamma p}(s, 0) \quad (7)$$

at large  $s_{\gamma p}$  and small  $Q^2$  with the same value of  $M_0^2$  in both Eqs.(2) and (7). The SLAC and SMC low  $Q^2$  data was combined to obtain one proton and one deuteron point corresponding to each experiment. The combined SLAC data at low  $x$  and low  $Q^2$  exhibits a clear positive proton asymmetry  $A_1^p = +0.077 \pm 0.016$  at  $\langle \sqrt{s_{\gamma p}} \rangle = 3.5 \text{ GeV}$  and  $\langle Q^2 \rangle = 0.45 \text{ GeV}^2$  while the deuteron asymmetry  $A_1^d = +0.008 \pm 0.022$  is consistent with zero. The small isoscalar deuteron asymmetry  $A_1^d$  indicates that the isoscalar contribution to  $A_1^p$  in the E-143 data is unlikely to be more than 30%. At larger  $\langle \sqrt{s_{\gamma p}} \rangle = 16.7 \text{ GeV}$  the SMC proton and deuteron low  $Q^2$  asymmetries are both consistent with zero:  $A_1^p = +0.011 \pm 0.013$  and  $A_1^d = +0.002 \pm 0.014$  at a mean  $\langle Q^2 \rangle = 0.45 \text{ GeV}^2$ . For the total photoproduction cross-section we took

$$(\sigma_A + \sigma_P) = 67.7 s_{\gamma p}^{+0.0808} + 129 s_{\gamma p}^{-0.4545} \quad (8)$$

(in units of  $\mu\text{b}$ ), which is known to provide a good Regge fit for  $\sqrt{s_{\gamma p}}$  between 2.5 GeV and 250 GeV [53]. (Here, the  $s_{\gamma p}^{+0.0808}$  contribution is associated with pomeron exchange and the  $s_{\gamma p}^{-0.4545}$  contribution is associated with the isoscalar  $\omega$  and isovector  $\rho$  trajectories.) Assuming a  $Q^2$ -independent  $A_1$  we combined Eqs.(4) and (8) to make various Regge fits through the SLAC proton point, which exhibits the only significant signal among the SLAC and SMC proton and deuteron low  $x$  low  $Q^2$  asymmetries. For definiteness we take  $\mu^2 = 0.5 \text{ GeV}^2$  in (4).

In Fig. 2 we show the asymmetry  $A_1^p$  as a function of  $\sqrt{s_{\gamma p}}$  between 2.5 and 250 GeV for the four different would-be Regge behaviours for  $(\sigma_A - \sigma_P)$ : that the high energy behaviour of  $(\sigma_A - \sigma_P)$  is given

- (a) entirely by the  $(a_1, f_1)$  terms in Equ.(4) with Regge intercept  $-\frac{1}{2}$  (conventional)
- (b) entirely by the  $(a_1, f_1)$  terms in Equ.(4) with Regge intercept  $+\frac{1}{2}$  (motivated by the observed small  $x$  behaviour of  $g_1^{(p-n)}$  in Eq.(6)),
- (c) by taking 2/3 isovector (conventional)  $a_1$  and 1/3 two non-perturbative gluon exchange contributions at  $\sqrt{s_{\gamma p}} = 3.5 \text{ GeV}$ ,
- (d) by taking 2/3 isovector (conventional)  $a_1$  and 1/3 pomeron-pomeron cut contributions at  $\sqrt{s_{\gamma p}} = 3.5 \text{ GeV}$ .

Polarized HERA could measure the real-photon spin asymmetry  $A_1$  for  $\sqrt{s_{\gamma p}}$  between 60 and 280 GeV to precision  $\delta A_1 \simeq 0.0003 - 0.0001$ ; eRHIC to precision  $\delta A_1 \simeq 0.0001 - 0.00003$  for  $\sqrt{s_{\gamma p}}$  between 20 and 90 GeV — see Section 3 and [51].

This polarized photoproduction measurement will help to constrain our understanding of spin-dependent Regge theory and to put an upper bound on the high-energy part of the Drell-Hearn-Gerasimov sum-rule. Given the projected asymmetries, Polarized HERA with  $\delta A_1 = 0.0003$  would be sensitive to  $(\sigma_A - \sigma_P)$  falling no faster than about  $s_{\gamma p}^{-1}$  ( $\alpha_{a_1} = 0$ ) at  $\sqrt{s_{\gamma p}} = 60\text{GeV}$ . For eRHIC with  $\delta A_1 = 0.0001$  one is sensitive to  $(\sigma_A - \sigma_P)$  falling no faster than about  $s_{\gamma p}^{-1.9}$  ( $\alpha_{a_1} = -0.9$ ) at the lower energy  $\sqrt{s_{\gamma p}} = 20\text{GeV}$ , which is well within all theoretical expectations for the large  $s_{\gamma p}$  behaviour of the asymmetry. At the upper energy  $\sqrt{s_{\gamma p}} = 90\text{GeV}$  one expects to see a signal for  $(\sigma_A - \sigma_P)$  falling no faster than about  $s_{\gamma p}^{-1}$  ( $\alpha_{a_1} = 0$ ).

## 4.2 Low $Q^2$ Region

Polarized eRHIC and HERA could measure the  $\gamma^*p$  spin asymmetry in the transition region ( $0.05 < Q^2 < 1\text{GeV}^2$ ) to precision  $\delta A_1 \simeq 0.00015$  and  $0.002$  respectively — see Section 3. At eRHIC the values of  $x$  are typically 10 times larger than for HERA for the same value of  $Q^2$ .

In Table 1 we estimate the size that  $g_1$  has to be in order to see a signal in each of practical  $(\sqrt{s_{\gamma p}}, Q^2)$  bins for the Polarized HERA and eRHIC Colliders. In a first approximation we take  $F_L = 0$  and use the ZEUS fit, Eq.(2), to  $F_2$  at low  $Q^2$  to calculate  $g_1 = \delta A_1 F_2/2x$ <sup>1</sup>. For  $\delta A_1$  we take the values as determined in Section 3. These  $g_1$  values are about a factor 10 (HERA) or even 100 (eRHIC) smaller the estimations for  $g_1$  at  $10\text{GeV}^2$  in the same range of  $x$ , which follow from extrapolating a QCD fit [8] to present  $g_1$  data from DESY, SLAC and SMC. Hence if the asymmetries follow the perturbative predictions down to  $Q^2 = 1\text{GeV}^2$ , both colliders will observe measurable asymmetries already after a small fraction of the data samples are collected.

Depending on the size of  $g_1$  at these low values of  $x$ , which remains to be measured, it is very likely to be possible to observe how the effective intercepts for  $g_1^{(p-n)}$  and  $g_1^{(p+n)}$  evolve with  $Q^2$  in the lower  $Q^2$  region. If the spin asymmetry  $A_1$  is indeed  $Q^2$  independent up to  $Q^2 \simeq 0.5\text{GeV}^2$ , then taking the asymmetry estimates in Fig. 2 one would expect to see a signal with eRHIC at  $\sqrt{s_{\gamma p}} \simeq 38\text{GeV}$  if  $g_1$  is less convergent than about  $g_1 \sim x^{0.3}$  as  $x \rightarrow 0$  with fixed  $Q^2 < 0.5\text{GeV}^2$ . For Polarized HERA with  $\delta A_1 = 0.002$  there will, most likely, be no definite signal if  $g_1$  follows the Regge behaviour  $g_1 \rightarrow 0$  when  $x \rightarrow 0$  at fixed low  $Q^2$ . If  $|g_1|$  at low fixed- $Q^2$  rises at small  $x$ , possibly due to significant gluonic  $\ln x$  or  $1/x \ln^2 x$  contributions, one could expect a measurable low  $Q^2$  asymmetry in both colliders. Experimentally, the strategy should be to measure  $A$  at low  $x$  with decreasing  $Q^2$  until the asymmetry becomes too small to be significant. The further one can probe into the transition

---

<sup>1</sup> Errors on  $F_2$  for HERA and eRHIC will be typically of the order of a few %, making  $\delta A_1$  by far the major source of experimental error.

$Q^2$					
	0.05	0.1	0.2	0.5	1.0
Polarized HERA with $\delta A_1 = 0.002$					
$\sqrt{s_{\gamma p}} (y)$					
120 (0.16)	$(3.5 \times 10^{-6}, 19)$	$(6.9 \times 10^{-6}, 18)$	$(1.4 \times 10^{-5}, 15)$	$(3.5 \times 10^{-5}, 11)$	$(6.9 \times 10^{-5}, 7)$
150 (0.25)	$(2.2 \times 10^{-6}, 31)$	$(4.4 \times 10^{-6}, 28)$	$(8.9 \times 10^{-6}, 24)$	$(2.2 \times 10^{-5}, 17)$	$(4.4 \times 10^{-5}, 12)$
190 (0.4)	$(1.4 \times 10^{-6}, 51)$	$(2.8 \times 10^{-6}, 47)$	$(5.5 \times 10^{-6}, 41)$	$(1.4 \times 10^{-5}, 29)$	$(2.8 \times 10^{-5}, 20)$
230 (0.6)	$(9.5 \times 10^{-7}, 79)$	$(1.9 \times 10^{-6}, 73)$	$(3.8 \times 10^{-6}, 63)$	$(9.5 \times 10^{-6}, 45)$	$(1.9 \times 10^{-5}, 30)$
Polarized eRHIC with $\delta A_1 = 0.00015$					
38 (0.14)	$(3.5 \times 10^{-5}, 0.12)$	$(6.9 \times 10^{-5}, 0.11)$	$(1.4 \times 10^{-4}, 0.09)$	$(3.5 \times 10^{-4}, 0.07)$	$(6.9 \times 10^{-4}, 0.04)$
47.5 (0.23)	$(2.2 \times 10^{-5}, 0.19)$	$(4.4 \times 10^{-5}, 0.18)$	$(8.9 \times 10^{-5}, 0.15)$	$(2.2 \times 10^{-4}, 0.11)$	$(4.4 \times 10^{-4}, 0.07)$
60 (0.36)	$(1.4 \times 10^{-5}, 0.32)$	$(2.8 \times 10^{-5}, 0.29)$	$(5.5 \times 10^{-5}, 0.26)$	$(1.4 \times 10^{-4}, 0.18)$	$(2.8 \times 10^{-4}, 0.12)$
72.5 (0.53)	$(9.5 \times 10^{-6}, 0.48)$	$(1.9 \times 10^{-5}, 0.44)$	$(3.8 \times 10^{-5}, 0.38)$	$(9.5 \times 10^{-5}, 0.27)$	$(1.9 \times 10^{-4}, 0.18)$

Table 1: The values  $(x, g_1 = \delta A_1 F_2 / 2x)$  for each of the practical  $(\sqrt{s_{\gamma p}}, Q^2)$  bins for Polarized HERA and eRHIC. Note that  $x$  is a factor of 10 higher for each  $Q^2$  bin compared to the HERA binning.

region, the greater the constraints one can provide on models of the Regge to hard  $Q^2$  transition at small  $x$ .

## 5 Conclusions

Exploration of the transition region between polarized photoproduction and deep inelastic scattering,  $0 < Q^2 < 1 \text{ GeV}^2$ , looks feasible with Polarized HERA and eRHIC. Polarized photoproduction measurements at these colliders would constrain our knowledge of spin dependent Regge theory and put an upper bound on the high-energy Regge contribution to the Drell-Hearn-Gerasimov sum-rule. Much larger changes in the effective intercept for the spin dependent structure function  $g_1$  at small  $x$  than for spin independent  $F_2$  are expected. A dedicated measurement at Polarized eRHIC or HERA would impose new constraints on QCD based models of the transition from Regge theory to perturbative QCD with increasing  $Q^2$  at fixed low  $x$ .

HERA and eRHIC will cover complementary regions in kinematics for these measurements, and will thus both provide important information. The potential high luminosity at eRHIC is certainly an advantage, and allows to reach high sensitivities in the transition region. Furthermore, it may be experimentally easier to reach lower  $Q^2$  with eRHIC. HERA will need again dedicated detectors to access the low  $Q^2$

region after the luminosity upgrade. With appropriate small angle tagging detectors in both the electron and proton direction, very precise data on asymmetries can be collected, which will be important in the progress of this data driven field to the study of the strong interaction. Hence, having such detector coverage included in design of a new detector for measuring  $ep$  and  $eA$  collisions at eRHIC is strongly encouraged. The use of deuteron beams with spectator tagging can help to disentangle different exchange contributions in the Regge regime.

### Acknowledgements

It is a pleasure to thank B. Badelek, D. Barber, A. Deshpande, G. Hofstatter, S. Levonian and G. Rädcl for helpful discussions. SDB acknowledges the hospitality of the CERN Theoretical Physics Division where this work was begun. This work was supported in part by BMBF and DFG.

### References

- [1] A. Donnachie and P.V. Landshoff, Z Physik **C61** (1994) 139.
- [2] M. Glück, E. Reya and A. Vogt, Eur. Phys. J. **C5** (1998) 461.
- [3] G. Altarelli and G. Parisi, Nucl. Phys. **B126** (1977) 298;  
V.N. Gribov and L. Lipatov, Sov. J. Nucl. Phys. **15** (1972) 438;  
L. Lipatov, Sov. J. Nucl. Phys. **20** (1975) 94;  
Y. Dokshitzer, Sov. Phys. JETP **46** (1977) 641.
- [4] A.M. Cooper-Sarkar, R.C.E. Devenish and A. De Roeck, Int. J. Mod. Phys. **A13** (1998) 3385.
- [5] B. Badelek and J. Kwiecinski, Rev. Mod. Phys. **68** (1996) 445;  
A. Donnachie, P.V. Landshoff, Phys. Lett. **B437** (1998) 408;  
H. Abramowicz, A. Levy, DESY-97-251 (1997);  
P. Desgrolard, L. Jenkovszky, F. Paccanoni, Eur. Phys. J. **C7** (1999) 263;  
K. Adel, F. Barriero and F.J. Yndurain, Nucl. Phys. **B495** (1997) 221;  
A. Capella et al., Phys. Lett. **B337** (1994) 358;  
D. Schildknecht, H. Spiesberger, hep-ph/9707447 (1997);  
Many contributions in Proceedings of DIS 1999 (Zeuthen), DIS 2000 (Liverpool).

- [6] Physics with Polarized Protons at HERA, eds. A. De Roeck and T. Gehrmann, DESY-PROC-1998-01;  
Polarized Protons at High Energies – Accelerator Challenges and Physics Opportunities, eds. A. De Roeck, D. Barber and G. Rädcl, DESY-PROC-1999-03.
- [7] See <http://quark.phy.bnl.gov/~raju/eRHIC.html>.
- [8] A. De Roeck, A. Deshpande, V.W. Hughes, J. Lichtenstadt and G. Rädcl, Eur. Phys. J **C6** (1999) 121.
- [9] S.D. Drell and A.C. Hearn, Phys. Rev. Lett. **162** (1966) 1520;  
S.B. Gerasimov, Yad. Fiz. **2** (1965) 839.
- [10] The H1 Collaboration (C. Adloff et al.), Nucl. Phys. **B497** (1997) 3.
- [11] The ZEUS Collaboration (J. Breitweg et al.), Eur. Phys. J **C7** (1999) 609.
- [12] The ZEUS Collaboration (J. Breitweg et al.), DESY preprint DESY-00-071, hep-ex/0005018.
- [13] P. Desgrolard, L. Jenkovszky, A. Lengyel, F. Paccanoni Phys. Lett. **B459** (1999) 265.
- [14] R.L. Heimann, Nucl. Phys. **B64** (1973) 429.
- [15] J. Ellis and M. Karliner, Phys. Lett. **B213** (1988) 73.
- [16] F.E. Close and R.G. Roberts, Phys. Lett. **B336** (1994) 257.
- [17] S.D. Bass and P.V. Landshoff, Phys. Lett. **B336** (1994) 537.
- [18] F.E. Close and R.G. Roberts, Phys. Rev. Lett. **60** (1988) 1471;  
L. Galfi, J. Kuti and A. Patkos, Phys. Lett. **B31** (1970) 465.
- [19] P.V. Landshoff and O. Nachtmann, Z Physik **C35** (1987) 405;  
J.R. Cudell, A. Donnachie and P.V. Landshoff, Nucl. Phys. **B322** (1989) 55.
- [20] J. Kuti, Erice lectures (1995), *in* Proc. Erice School *The spin structure of the nucleon*, eds. B. Frois, V. Hughes and N. de Groot (World Scientific, 1997).
- [21] S.D. Bass, Mod. Phys. Lett. **A12** (1997) 1051.
- [22] S.D. Bass and M.M. Brisudova, Eur. Phys. J **A4** (1999) 251.
- [23] N. Bianchi and E. Thomas, Phys. Lett. **B450** (1999) 439.
- [24] B. Lampe and E. Reya, Phys. Rept. **332** (2000) 1.

- [25] M. Gluck, E. Reya, M. Stratmann and W. Vogelsang, Phys. Rev. **D53** (1996) 4775.
- [26] T. Gehrmann and W.J. Stirling, Phys. Rev. **D53** (1996) 6100.
- [27] G. Altarelli, R.D. Ball, S. Forte and G. Ridolfi, Nucl. Phys. **B496** (1997) 337.
- [28] J. Bartels, B.I. Ermolaev and M.G. Ryskin, Z Phys **C70** (1996) 273; **C72** (1996) 627.
- [29] J. Blümlein and A. Vogt, Phys. Lett. **B386** (1996) 350.
- [30] Y. Kiyo, J. Kodaira and H. Tochimura, Z. Phys. **C74** (1997) 631.
- [31] J. Kwiecinski and B. Ziaja, Phys. Rev. **D60** (1999) 054004;  
B. Badelek and J. Kwiecinski, Phys. Lett. **B418** (1998) 229;  
B. Badelek, J. Kiriyluk and J. Kwiecinski, Phys. Rev. **D61** (2000) 014009.
- [32] The New Muon Collaboration (M. Arneodo et al.), Phys. Rev. **D50** (1994) R1;  
Nucl. Phys. **B483** (1997) 3.
- [33] The Spin Muon Collaboration (B. Adeva et al), Phys. Rev. **D58** (1998) 112001.
- [34] The E-143 Collaboration (K. Abe et al.), Phys. Rev. Lett. **74** (1995) 346; Phys. Rev. **D58** (1998) 112003.
- [35] The E-154 Collaboration (K. Abe et al.), Phys. Rev. Lett. **79** (1997) 26.
- [36] J. Soffer and O.V. Teryaev, Phys. Rev. **D56** (1997) 1549.
- [37] S.D. Bass, Eur. Phys. J **A5** (1999) 17.
- [38] J.D. Bjorken, Phys. Rev. **148** (1966) 1467; Phys. Rev. **D1** (1970) 1376.
- [39] A. A. Sokolov and I.M. Ternov, Sov. Phys. Dok. **8** (1964) 1203
- [40] D.P. Barber et al., Proceedings of the Workshop Future Physics at HERA, Eds. G. Ingelman, A. De Roeck, R. Klanner, (1996) 1205;  
SPIN at HERA Collaboration, L.V. Alekseeva et al., University of Michigan preprint UMHE-96-20 (1996)  
SPIN at HERA Collaboration, L.V. Alekseeva et al., University of Michigan preprint UMHE-99-05 (1999)
- [41] W. Bartel et al., proceedings of the workshop on 'Future Physics at HERA', Eds. G. Ingelman, A. De Roeck and R. Klanner, (1996) p. 1095.

- [42] A. Skrinsky, in proceedings of the workshop on Physics with a high luminosity polarized electron ion collider, Bloomington, April 1999, 26.  
Ya. S. Derbenev and V. A. Anferov, physics/0003104 (2000);  
G.H. Hoffstätter, Future possibilities for HERA”, Proceedings of the EPAC2000 conference, in preparation.
- [43] D. Barber, G.H. Hoffstätter and A. Zelenski, private communication.
- [44] M. Düren, in Proceedings of the Workshop on Future Physics at HERA, Eds. G. Ingelman, A. De Roeck and R. Klanner, DESY (1996) 854.
- [45] M. Krasny, in Proceedings of the 2nd eRHIC Workshop, Yale, April 2000.
- [46] H1 Collab., I. Abt et al., Nucl. Instr. and Meth. **A386** (1997) 310 and **A386** (1997) 348;  
V.F. Andreev et al., hep-ex/0008042.
- [47] C.F. Weizsäcker, Z. Phys. **88** (1934) 612;  
E.J. Williams, Phys. Rev. **45** (1934) 729.
- [48] ZEUS Collaboration, Contributed paper to the International Europhysics Conference on High Energy Physics 99, Tampere, Finland, paper 493.
- [49] H1 Collaboration, Technical proposal to built a special spectrometer covering very small momentum transfers, May 1996
- [50] R. Brinkman, in Proceedings of the Workshop on Future Physics at HERA, Eds. G. Ingelman, A. De Roeck and R. Klanner, DESY (1996) 1158.
- [51] S.D. Bass, M.M. Brisudova and A. De Roeck, hep-ph/9710518, in Proc. Physics with Polarized Protons at HERA, eds. A. De Roeck and T. Gehrmann, DESY-PROC-1998-01.
- [52] The E-143 Collaboration (K. Abe et al.), Phys. Lett. **B364** (1995) 61.
- [53] P.V. Landshoff, Proc. Zuo Summer School, PSI Proceedings 94-01 (1994) 135, hep-ph/9410250.



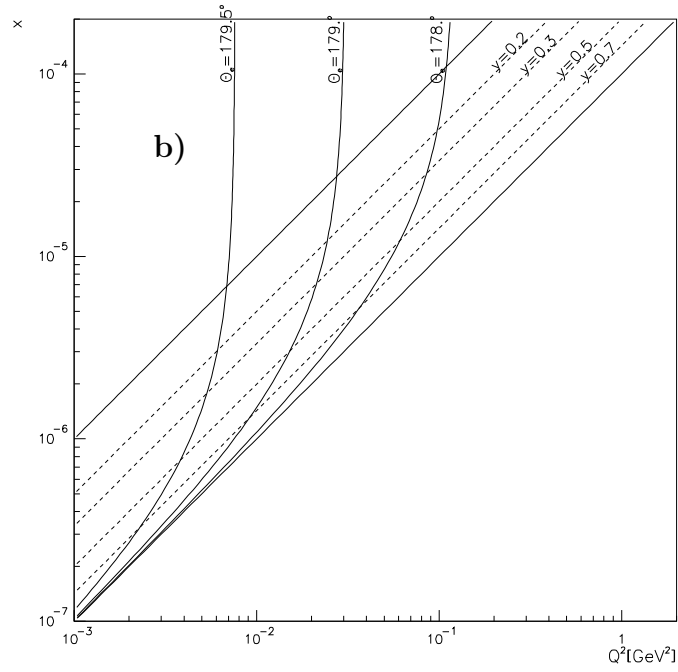
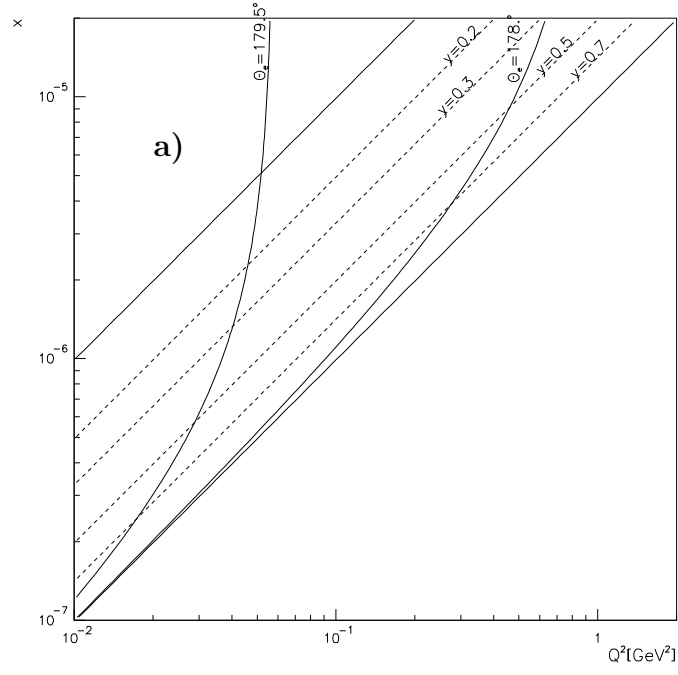


Figure 1: The kinematical region accessible by **a)** HERA and **b)** eRHIC. The angles are defined with respect to the proton beam direction.

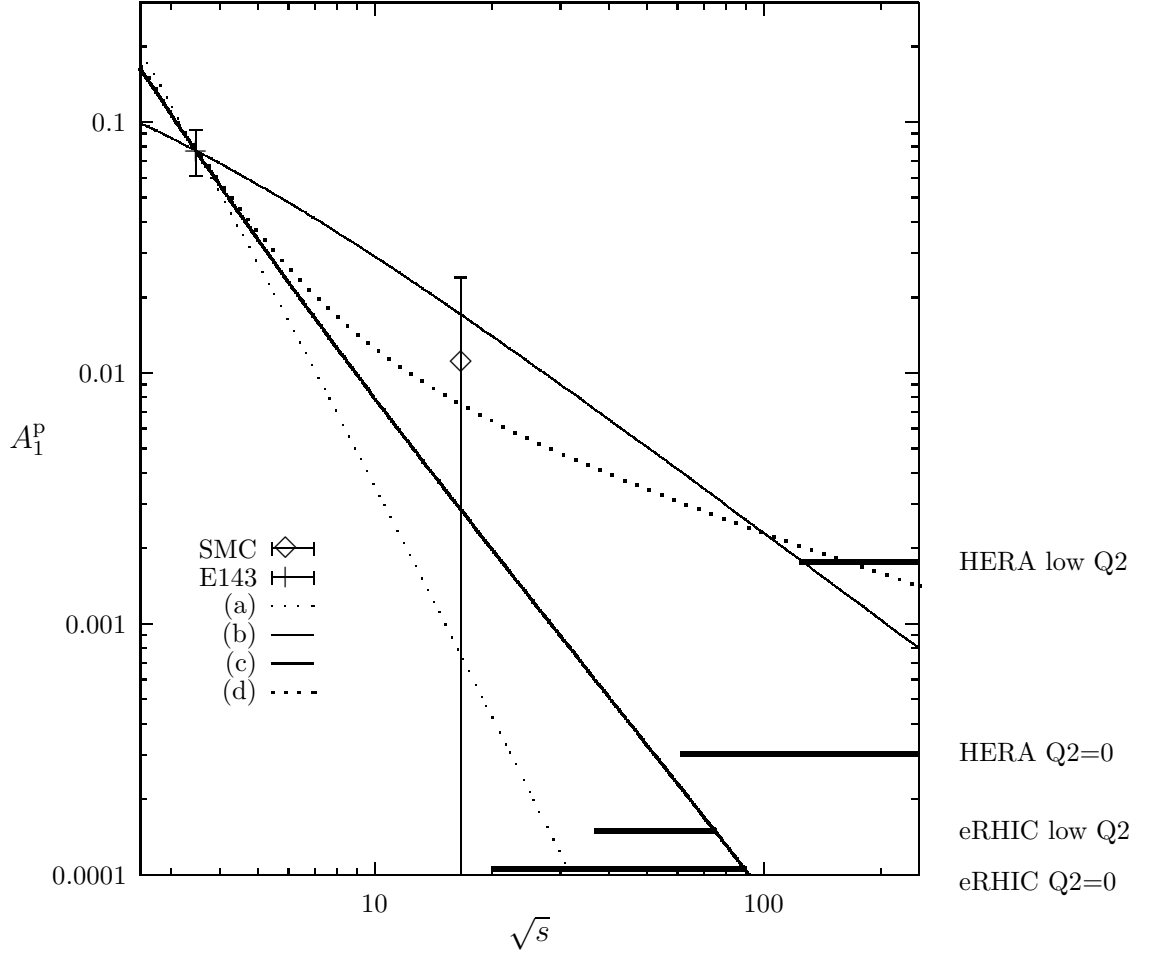


Figure 2: **The asymmetry**  $A_1^p$  as a function of  $\sqrt{s_{\gamma p}}$  for different Regge behaviours for  $(\sigma_A - \sigma_P)$ : given entirely by (a) the  $(a_1, f_1)$  terms in Eq.(4) with Regge intercept either  $-\frac{1}{2}$  (conventional) or (b)  $+\frac{1}{2}$  (c) by 2/3 isovector (conventional)  $a_1$  and 1/3 two non-perturbative gluon exchange contributions at  $\sqrt{s} = 3.5\text{GeV}$ ; (d) by 2/3 isovector (conventional)  $a_1$  and 1/3 pomeron-pomeron cut contributions at  $\sqrt{s} = 3.5\text{GeV}$ . The solid horizontal lines indicate the kinematic range and precision of the Polarized eRHIC and HERA colliders at low  $Q^2$ .